Title
Regional cerebral blood flow alterations in obstructive sleep apnea

Authors
Yadav, Santosh K
Kumar, Rajesh
Macey, Paul M
et al.

Publication Date
2013-10-01

DOI
10.1016/j.neulet.2013.09.033

Peer reviewed

Neuroscience Letters 555 (2013) 159–164

Contents lists available at ScienceDirect

Neuroscience Letters

journal homepage: www.elsevier.com/locate/neulet

Regional cerebral blood flow alterations in obstructive sleep apnea

Santosh K. Yadav[a], Rajesh Kumar[a,*], Paul M. Macey[b], Heidi L. Richardson[a], Danny J.J. Wang[c], Mary A. Woo[b], Ronald M. Harper[a,d]

[a] Department of Neurobiology, University of California at Los Angeles, Los Angeles, CA 90095, USA
[b] UCLA School of Nursing, University of California at Los Angeles, Los Angeles, CA 90095, USA
[c] Department of Neurology, David Geffen School of Medicine at UCLA, University of California at Los Angeles, Los Angeles, CA 90095, USA
[d] Brain Research Institute, University of California at Los Angeles, Los Angeles, CA 90095, USA

HIGHLIGHTS

- Regional cerebral blood flow (CBF) was examined in obstructive sleep apnea.
- Values were significantly reduced, principally in major sensory and motor fiber systems.
- Reduced CBF may contribute to upper airway and diaphragm coordination loss.
- The reduced regional flow may lead to further neural damage in the syndrome.

ARTICLE INFO

Article history:
Received 29 June 2013
Received in revised form
12 September 2013
Accepted 14 September 2013

Keywords:
Arterial spin labeling
Cerebral hemodynamics
Motor coordination
Sensory control
Hypoxemia

ABSTRACT

Obstructive sleep apnea (OSA) is a condition characterized by upper airway muscle atonia with continued diaphragmatic efforts, resulting in repeated airway obstructions, periods of intermittent hypoxia, large thoracic pressure changes, and substantial shifts in arterial pressure with breathing cessation and resumption. The hypoxic exposure and hemodynamic changes likely induce the structural and functional deficits found in multiple brain areas, as shown by magnetic resonance imaging (MRI) procedures. Altered cerebral blood flow (CBF) may contribute to these localized deficits; thus, we examined regional CBF, using arterial spin labeling procedures, in 11 OSA (age, 49.1 ± 12.2 years; 7 male) and 16 control subjects (42.3 ± 10.2 years; 6 male) with a 3.0-Tesla MRI scanner. CBF maps were calculated, normalized to a common space, and regional CBF values across the brain quantified. Lowered CBF values emerged near multiple bilateral brain sites in OSA, including the corticospinal tracts, superior cerebellar peduncles, and pontocerebellar fibers. Lateralized, decreased CBF appeared near the left inferior cerebellar peduncles, left tapetum, left dorsal fornix/stria terminalis, right medial lemniscus, right red nucleus, right midbrain, and midline pons. Regional CBF values in OSA are significantly reduced in major sensory and motor fiber systems and motor regulatory sites, especially in structures mediating motor coordination; those reductions are often lateralized. The asymmetric CBF declines in motor regulatory areas may contribute to loss of coordination between upper airway and diaphragmatic musculature, and lead to further damage in the syndrome.

1. Introduction

Obstructive sleep apnea (OSA) is defined by interrupted breathing during sleep from repeated upper airway obstructions while diaphragmatic efforts continue, resulting in intermittent hypoxemia, repetitive arousals, and disruption of normal sleep architecture [10]. A principal OSA characteristic is a loss of coordination of the breathing musculature, with atonia of genioglossal and other upper airway muscles in the presence of active diaphragmatic movements.

Routine magnetic resonance imaging (MRI) in OSA, upon visual examination, shows no gross brain pathology, except white matter infarcts or cerebellar changes [9]. However, voxel-based morphometry and manual volumetric procedures using high-resolution T1-weighted images, T2-relaxometry, and diffusion tensor imaging-based indices, show gray and white matter changes in autonomic, breathing, mood and anxiety, and cognitive control

Abbreviations: OSA, obstructive sleep apnea; CBF, cerebral blood flow; ASL, arterial spin labeling; MRI, magnetic resonance imaging; TR, repetition time; TE, echo-time; FOV, field of view; FA, flip-angle; EPI, echo-planner-imaging.

* Corresponding author at: Department of Neurobiology, David Geffen School of Medicine at UCLA, University of California at Los Angeles, Los Angeles, CA 90095-1763, USA. Tel.: +1 310 206 1679; fax: +1 310 825 2224.
E-mail address: rkumar@mednet.ucla.edu (R. Kumar).

0304-3940/$ – see front matter © 2013 Elsevier Ireland Ltd. All rights reserved.
http://dx.doi.org/10.1016/j.neulet.2013.09.033

sites [19,20,23]. Functional deficits within structurally damaged areas, based on functional MRI procedures, also appear in OSA during autonomic and respiratory challenges in regions that control autonomic, breathing, and cognitive functions [15]. The processes contributing to brain injury and associated altered brain function are unknown, but may include aberrant local perfusion changes, induced by frequent hypoxic episodes, blood pressure surges, failure of cerebral autoregulation, or endothelial changes induced by epigenetic processes [17].

Reduced cerebral blood flow (CBF) appears in OSA, based on imaging procedures with relatively limited resolution. Decreased CBF values emerge in various brain areas of awake OSA subjects assessed by transcranial Doppler [34], and single photon emission computed tomography procedures [12], and during sleep, as well as wakefulness states, as evaluated by tracer-based computerized tomography [25]. However, precise assessment of localized CBF changes in areas damaged in OSA is lacking.

Arterial spin labeling (ASL) procedures are non-invasive MRI-based methods that quantify regional CBF values with greater sensitivity and specificity than Doppler techniques [4,14,32], and provide whole brain CBF values more rapidly than Doppler procedures. ASL-based CBF measurements take advantage of arterial water as a freely diffusible tracer, and do not require use of contrast agents [11]. The procedure has been used to quantify regional CBF changes in different disease conditions [3,11], and to monitor disease progression [3], and treatment effects. The technique may assist precise examination of regional CBF changes in OSA subjects.

Our aim was to assess localized CBF changes in OSA over control subjects using non-invasive ASL procedures. We hypothesized that regional CBF values would be altered in OSA, in brain sites that showed structural injury earlier in the condition.

2. Materials and methods

2.1. Subjects

We studied 11 OSA (age, 49.1 ± 12.2 years; body-mass-index, 28.3 ± 4.0 kg/m^2; apnea-hypopnea-index, 32.9 ± 16.6 events/h; education, 18.5 ± 2.4 years; 7 male) and 16 control subjects (age, 42.3 ± 10.2 years; body-mass-index, 24.1 ± 3.7 kg/m^2; education, 16.9 ± 4.4 years; 6 male). No participants were taking cardiovascular-altering medications, such as β-blockers, α-agonists, angiotensin-converting enzyme inhibitors, or vasodilators, or any mood changing drugs, such as selective serotonin reuptake inhibitors. Subjects with any history of heart failure, stroke, diagnosed cerebral conditions, metallic implants, or body weight more than 125 kg (scanner limitation) were excluded. Control subjects were healthy and without any medications that might alter brain structure or hemodynamics, and with no contraindications to the MRI scanner. All procedures were approved by the Institutional Review Board at University of California at Los Angeles, and each subject provided written informed consent prior to study.

2.2. Magnetic resonance imaging

Brain studies were performed on a 3.0-Tesla MRI scanner (Siemens, Magnetom, Tim-Trio, Erlangen, Germany). Subjects lay supine, awake, and breathed normally during scans. High-resolution T1-weighted images were collected using the magnetization-prepared-rapid-acquisition-gradient-echo pulse sequence [repetition time (TR) = 2200 ms, echo-time (TE) = 2.34 ms, inversion time = 900 ms, flip-angle (FA) = 9°, 320 × 320 matrix size, 230 mm × 230 mm field of view (FOV), 0.9 mm slice thickness, and 192 sagittal slices]. Proton-density and T2-weighted images were collected using a dual-echo turbo spin-echo pulse sequence in the axial plane (TR = 10,000 ms, TE1,2 = 17, 134 ms, FA = 130°, 256 × 256 matrix size, 230 mm × 230 mm FOV, 3.0 mm slice thickness, and ∼56 slices). ASL imaging was performed using a pseudocontinuous ASL pulse sequence in the axial plane (TR = 4000 ms, TE = 11 ms, FA = 90°, bandwidth = 3004 Hz/pixel, label offset = 90 mm, label-delay = 1200 ms, 64 × 64 matrix size, 230 mm × 230 mm FOV, 3.5 mm slice thickness, 20% distance factor, 38 axial slices, and 100 repeats).

2.3. Data processing and analysis

T1-weighted, proton-density, and T2-weighted images were visually assessed for any gross brain pathology, including infarcts, cystic lesions, and tumors, before data processing. ASL data were also examined for any potential motion or imaging artifacts.

2.4. Calculation of CBF maps

Using MATLAB-based custom software, whole-brain CBF maps were calculated. Labeled and non-labeled ASL brain volumes were realigned to remove any potential head-motion related artifacts; both non-labeled and labeled images were aligned to the first image. Using the realigned echo-planner-imaging (EPI) scans, perfusion images were calculated with simple subtraction from non-labeled to labeled images. Perfusion images were used to calculate CBF maps (units, ml/100 g/min), based on a modified single-compartment ASL perfusion model [35]. The non-labeled EPI scans and CBF maps were averaged across the series to derive mean EPI scan and CBF map per individual subject.

2.5. Normalization of CBF maps and regional analyses

SPM8 software (www.fil.ion.ucl.ac.uk/spm) was used to strip skulls from the individual CBF maps using the corresponding EPI images. Subsequent normalization of CBF maps to a common space was performed using linear affine and non-linear transformation procedures (www.mristudio.org). Both EPI images and CBF maps were first normalized to the JHU_MNI_SS_b0 "Eve" atlas, a single-subject template in the Montreal Neurological Institute (MNI) common space, using a linear affine transformation with trilinear interpolation. After linear transformation of EPI images and CBF maps to the MNI common space, a single-channel large deformation diffeomorphic metric mapping transformation approach was used for non-linear transformation to the MNI space. Non-linear transformed matrices were obtained with cascading alpha values, and then parameters from transformation matrices were applied to both mean EPI images and CBF maps [29]. The resulting transformed CBF maps were used to automatically quantify mean regional CBF values from whole-brain structures using region of interest (ROI) editor software.

2.6. Statistical analysis

The IBM statistical package for the social sciences (IBM SPSS Statistics 20) was used to assess demographics and regional CBF values. Demographic data were examined with independent samples *t*-tests and Chi-square. Regional CBF values were assessed with independent samples *t*-tests (statistical threshold of $p \leq 0.05$).

3. Results

3.1. Demographics

No significant differences were observed between groups in age ($p = 0.13$), gender ($p = 0.18$), or education ($p = 0.38$). However,

Table 1
Average CBF values (ml/100 g/min) from different brain regions in OSA and control subjects.

Brain regions	OSA ($n = 11$) (mean ± SD)	Controls ($n = 16$) (mean ± SD)	p values
Right insula	51.7 ± 7.0	53.9 ± 10.1	0.581
Left insula	48.3 ± 10.7	55.9 ± 10.2	0.074
Right cerebellum	39.9 ± 12.8	47.6 ± 8.5	0.076
Left cerebellum	38.9 ± 12.6	46.5 ± 8.7	0.075
*Right corticospinal tract	34.6 ± 8.5	46.9 ± 12.5	0.009
*Left corticospinal tract	35.1 ± 9.9	44.4 ± 11.2	0.038
Right inferior cerebellar peduncle	33.3 ± 10.2	39.7 ± 12.9	0.181
*Left inferior cerebellar peduncle	28.8 ± 9.4	39.3 ± 11.8	0.023
*Right superior cerebellar peduncle	32.2 ± 10.3	44.8 ± 13.6	0.016
*Left superior cerebellar peduncle	35.9 ± 10.4	45.9 ± 11.7	0.031
*Right medial lemniscus	36.9 ± 8.1	50.5 ± 16.2	0.017
Left medial lemniscus	37.8 ± 10.6	47.2 ± 16.2	0.100
Right cingulum, cingulate gyrus	30.9 ± 2.7	34.5 ± 6.2	0.056
Left cingulum, cingulate gyrus	28.8 ± 4.01	29.9 ± 5.8	0.574
Right dorsal fornix/stria terminalis	40.7 ± 12.3	40.6 ± 7.8	0.990
*Left dorsal fornix/stria terminalis	36.6 ± 10.9	45.8 ± 7.7	0.017
*Right pontocerebellar fibers	38.4 ± 10.6	54.4 ± 17	0.011
*Left pontocerebellar fibers	37.4 ± 11.3	49.0 ± 16	0.049
*Right red nucleus	36.6 ± 11.7	52.3 ± 16.2	0.012
Left red nucleus	35.3 ± 15.6	46.5 ± 15.5	0.077
Right tapetum	16.8 ± 12	20.1 ± 9.2	0.435
*Left tapetum	13.7 ± 6.1	20.4 ± 9.2	0.045
*Right midbrain	36.6 ± 8.9	44.0 ± 9.3	0.050
Left midbrain	36.9 ± 9.2	43.8 ± 9.0	0.064
*Midline pons	40.6 ± 9.0	54.5 ± 15.2	0.012
Left fronto-orbital gyrus	35.2 ± 10.7	37.1 ± 8.9	0.085
Right fronto-orbital gyrus	50.3 ± 14.2	53.1 ± 8.5	0.523

CBF, cerebral blood flow; OSA, obstructive sleep apnea; SD, standard deviation.
* Significant at $p \leq 0.05$.

body-mass-indices were significantly increased in OSA over controls ($p = 0.01$).

3.2. Regional CBF changes in OSA

Significantly reduced regional CBF values appeared near multiple brain areas in OSA compared to control subjects (Table 1 and Fig. 1A), but no sites showed significantly increased localized values in OSA over controls. Examples of whole-brain CBF maps from an OSA and a control subject are shown in Fig. 1B. Reduced CBF values in OSA appeared near the bilateral corticospinal tracts (right, $p = 0.009$; left, $p = 0.04$), superior cerebellar peduncles (right, $p = 0.02$; left, $p = 0.03$), and pontocerebellar fibers (right, $p = 0.01$; left, $p = 0.05$). However, unilateral reductions in CBF of OSA subjects appeared in the medial lemniscus (right, $p = 0.02$), red nucleus (right, $p = 0.012$), tapetum (left, $p = 0.04$), dorsal fornix/stria terminalis (left, $p = 0.02$), inferior cerebellar peduncle (left, $p = 0.02$), and midbrain (right, $p = 0.05$), compared to control subjects (Fig. 1A); reduced flow also appeared in the midline pons ($p = 0.01$).

4. Discussion

4.1. Overview

Significantly reduced regional CBF values appeared in the vasculature for multiple brain regions in OSA subjects, and many of these sites, including the red nucleus, corticospinal tracts, midline pons, and medial lemniscus, assist coordination of respiratory musculature, in addition to roles in other motoric functions. The cerebellar peduncles and pontocerebellar fibers similarly participate in motor coordination, as well as autonomic regulation; the tapetum and fornix fibers serve significant roles in memory and cognitive functions, and the stria terminalis is involved in stress and anxiety control.

The processes underlying the altered regional CBF values to those sites in OSA are unclear. However, the asymmetric nature of the altered flow, and the preferentially reduced CBF to motor regulatory and coordination areas, suggest that the reduced flow may contribute to the pathological respiratory motor coordination found in OSA, manifested as atonia of upper airway musculature occurring at times when activation prior to diaphragmatic muscle onset is required. Inadequate local perfusion would lead to failed or inadequate performance of sensory and motor coordination structures, here represented by the red nucleus, cerebellar pathway, corticospinal tracts, and medial lemniscus. The deficits could contribute to failed coordination of respiratory musculature.

4.2. OSA and cerebral hemodynamics

OSA subjects show profound overall CBF changes during apneas [12,25,34], and apnea-induced hypoxemia, combined with decreased cerebral perfusion, may lead to chronically altered CBF in OSA [2]. Resting arterial CBF is reduced in OSA, assessed by transcranial Doppler. We used advanced MRI-based ASL procedures that quantify regional CBF values with greater sensitivity and specificity than Doppler procedures [32]. Typically, Doppler procedures can provide 85% accuracy [14], while ASL techniques can provide up to 100% [4], relative to invasive radioactive tracer procedures. Also, Doppler procedures are operator-dependent, allow limited evaluation of only some brain vessels, e.g., middle cerebral arteries, are relatively low-resolution, and are very time-consuming over ASL techniques.

Other imaging procedures, including tracer-based computerized tomography, show decreased CBF in OSA in brainstem and cerebellar regions during wakefulness [25]. During sleep, OSA subjects exhibit decreased CBF in frontal, parietal, and occipital cortices, pons, and the cerebellum, based on single photon emission computed tomography procedures [12,25]. We extend these findings by demonstrating more-localized CBF changes in OSA.

4.3. CBF reduction and brain tissue changes

Animal models which examine the relationship between CBF reduction and brain tissue injury show that a 25 ml/100 g/min CBF

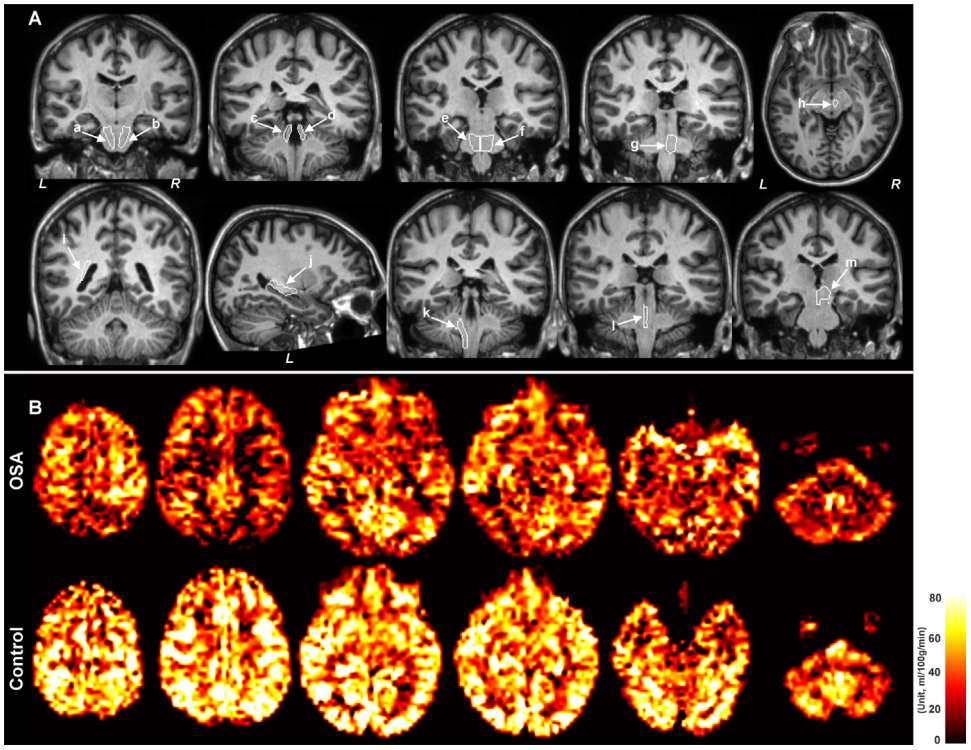

Fig. 1. (A) Regions of interest (ROIs) from different brain sites, overlaid onto T1-weighted images that showed significant bilateral and unilateral reduction of CBF in OSA. The bilateral areas included the corticospinal tracts (coronal; a, b), superior cerebellar peduncles (coronal; c, d), pontocerebellar fibers (coronal; e, f), and regions of unilateral CBF reduction, which included the right medial lemniscus (coronal; g), right red nucleus (axial; h), left tapetum (coronal; i), left dorsal fornix/stria terminalis (sagittal; j), left inferior cerebellar peduncle (coronal; k), midline pons (coronal; l), and right midbrain (coronal; m). All brain images are displayed in neurological convention, with the left side of brain represented on the left side of the image. (*L* = Left, *R* = right). (B) Examples of whole-brain CBF maps in an OSA (age, 55.7 years; male), and a control subject (age, 54.9 years; male). Warm colors indicate corresponding regional CBF values.

reduction leads to tissue infarcts in those areas [26]. In this study, we observed regional CBF reduction in several brain areas that ranged from 7 to 16 ml/100 g/min in resting conditions in OSA subjects. However, CBF reduction would be larger for those brain sites during sleep with apneic episodes, and of course, apneic periods occur hundreds of times during a night. We believe that lower CBF values in resting conditions, enhanced CBF reduction during apneic episodes, and multiple exposures to apnea would significantly contribute to tissue injury in OSA. Structural injury and functional deficits are now well-documented for various brain regions in OSA, and many of the brain areas with reduced regional CBF values found here overlap areas of injury. Since decreased flow will lead to brain injury, contributing to symptoms in the syndrome, interventions to address reduced CBF may be a useful target in OSA.

4.4. Altered brain functions and CBF changes

Coordination of the upper airway muscles with diaphragmatic activation is of special importance in breathing; effective airflow depends on activation of the genioglossal fibers of the tongue slightly before diaphragmatic descent to prevent airway collapse from excessive negative pressure. In OSA, that coordination is largely lost, with atonia of the upper airway muscles, followed by airway collapse. Atonia appears not to result from damage to the XII motor nucleus pool, since obstruction does not appear in wakefulness, and apparently reflects a sleep state influence on coordination between brainstem motor nuclei and the phrenic motor pool.

Coordination pathways and nuclei were especially affected in regional CBF declines. The right red nucleus, which projects contralaterally to the left cerebellum, and provides coordination for much of the automatic motor musculature, was affected, as were contralateral cerebellar projecting fibers. The corticospinal motor fibers were also impacted. In addition, areas within the midline pons, including the periaqueductal gray modulate respiratory and cardiovascular activity, demonstrated by single neuron discharge [27,28], and electrical stimulation evidence [5]. The medial lemniscus, the major somatosensory pathway from body structures, plays a significant role in motor coordination, and was affected [16]. The tapetum, forming part of the splenium of the corpus callosum, carries information for cognitive, and memory processes [22]. The hippocampus projects to the mammillary bodies and diencephalic structures through the fornix. The mammillary bodies show substantial volume loss, especially on the left side in OSA [19]; the reduced CBF to the dorsal left fornix may have contributed to that injury. The fornix fibers play a significant role in memory processes, by bridging hippocampal and mammillary structures [13], and the stria terminalis serves an important role in anxiety and stress [7]; all of these processes are deficient in OSA. Collectively, these pathways serve significant roles for upper airway motor coordination, memory and cognitive functions [1,19].

4.5. Factors contributing to reduced CBF

Several mechanisms may contribute to the localized reduction in CBF values in OSA. The condition damages the insular, cingulate, and medial frontal cortices, as well as the raphe and ventrolateral medulla [20,23], all essential brain areas for vascular regulation. The right insular, cingulate and medial frontal cortices exert significant influences on the sympathetic system [6], the raphe modulates vascular diameter [8], and the ventrolateral medulla is a final integrative site for sympathetic outflow [18]. Damage to these vascular regulatory sites may have contributed to the regional CBF deficits. The consequences of intermittent hypoxia to peripheral vascular

regulation are especially apparent in developing animals, where injury to peripheral sympathetic ganglia appears [38].

Intermittent hypoxia affects both neural tissue and the vasculature, and the substantial hemodynamic alterations during each apneic event, shifting systolic and diastolic arterial pressure up to 240/130 mmHg [31], can also contribute to vascular injury. Cerebellar tissue changes appear in animal models of OSA with as few as 5 h of 10% O_2 intermittent hypoxic exposure [30]. The cerebellum exerts significant influences on blood pressure regulation, shows substantial injury in OSA [23], and may contribute to the flawed vascular regulation here.

Normally, $PECO_2$ exerts a significant impact on the vasculature; vessels constrict and dilate in response to changes in $PECO_2$ concentration [37]. The potential blunting of vasodilation to $PECO_2$ in OSA is one more factor that may alter CBF. That consideration is made more complex by the injury to medullary and raphe systems in OSA, with raphe serotonergic neurons especially playing a significant role in mediation of CO_2 effects on the vasculature [36]. We earlier showed in a human model of CO_2 dysregulation, congenital central hypoventilation syndrome, that the vasculature was severely affected, particularly in the basilar arteries near the damaged raphe in those patients [21]. The medullary injury we previously reported for OSA may also interfere with CO_2 dilatory effects [20], although that possibility is entirely speculative.

Intermittent hypoxic exposure also affects endothelial cells, resulting in abnormal vascular activity [33]. Hypoxic exposure retracts the lateral junctions between adjacent endothelial cells through reduction in adenyl cyclase activity, leading to increased space between cells [7], affecting the barrier properties of the endothelium. Such alterations in the microvasculature can result in compromised hemodynamic activity, leading to altered regional CBF.

4.6. Limitations

Limitations of this study include the small sample size, potential variability of regional CBF values in OSA between genders, restricted spatial resolution, and normalization accuracy of post processing. Although various brain sites demonstrated significant group differences between OSA and control subjects, showing sufficient power in those areas, the limited number of subjects may have restricted the power to show group differences in rostral brain sites that exhibit structural brain injury in OSA subjects [19,20,23]. That aspect may be especially the case for the left insula and right cingulate cortex, which show substantial injury in OSA [20,23], but only showed a trend of lowered CBF here ($p = 0.07$, $p < 0.056$, respectively). Structural brain injury differences appear between genders in OSA subjects [24], but the small number of OSA subjects here restricted the ability to partition potential CBF differences induced by sex. The spatial resolution was limited due to technical limitations, and CBF values from smaller regional sites could have been contaminated from surrounding structures. The normalization process may introduce some inaccuracies, but CBF maps of all OSA and control subjects were visually inspected to verify only modest variation across subjects.

4.7. Conclusions

Regional CBF values were lower in unilateral and some bilateral brain sites in OSA, including major sensory and motor fiber systems and motor regulatory regions; the declines were especially apparent in fiber and nuclear systems responsible for motor coordination. The asymmetric nature of the reduced CBF in selected motor areas, affecting the right, but not left red nucleus, and the left cerebellar peduncles, has the potential to contribute to impaired coordination of the respiratory musculature. The origins of the altered regional CBF values remain unclear, but may result from early injury of vascular regulatory areas in OSA from intermittent hypoxia, or from the substantial hemodynamic changes that accompany the large thoracic pressure alterations during apneic periods. By failing to provide adequate CBF to these affected areas, the potential for even further brain tissue damage exists. Moreover, since coordination by cerebellar and other motor areas is essential for maintaining timely activation of the upper airway musculature relative to diaphragmatic discharge, reduction in CBF of those structures may worsen apnea characteristics.

Conflict of interest

All authors have no conflict of interest to declare.

Acknowledgements

Authors thank Ms. Rebecca Harper and Dr. Jenifer Ogren for assistance with data collection. This research was supported by the National Institutes of Health R01 HL113251 and R01 NR013693. HLR was supported by NHMRC CJ Martin Fellowship 606770.

References

[1] M.J. Aminoff, T.A. Sears, Spinal integration of segmental, cortical and breathing inputs to thoracic respiratory motoneurones, J. Physiol. 215 (1971) 557–575.
[2] E.M. Balfors, K.A. Franklin, Impairment of cerebral perfusion during obstructive sleep apneas, Am. J. Respir. Crit. Care Med. 150 (1994) 1587–1591.
[3] M.A. Binnewijzend, J.P. Kuijer, M.R. Benedictus, W.M. van der Flier, A.M. Wink, M.P. Wattjes, B.N. van Berckel, P. Scheltens, F. Barkhof, Cerebral blood flow measured with 3D pseudocontinuous arterial spin-labeling MR imaging in Alzheimer disease and mild cognitive impairment: a marker for disease severity, Radiology 267 (2013) 221–230.
[4] G.G. Brown, C. Clark, T.T. Liu, Measurement of cerebral perfusion with arterial spin labeling: Part 2. Applications, J. Int. Neuropsychol. Soc. 13 (2007) 526–538.
[5] P. Carrive, R. Bandler, R.A. Dampney, Anatomical evidence that hypertension associated with the defence reaction in the cat is mediated by a direct projection from a restricted portion of the midbrain periaqueductal grey to the subretrofacial nucleus of the medulla, Brain Res. 460 (1988) 339–345.
[6] D.F. Cechetto, S.J. Chen, Subcortical sites mediating sympathetic responses from insular cortex in rats, Am. J. Physiol. 258 (1990) R245–R255.
[7] D.C. Choi, A.R. Furay, N.K. Evanson, M.M. Ostrander, Y.M. Ulrich-Lai, J.P. Herman, Bed nucleus of the stria terminalis subregions differentially regulate hypothalamic–pituitary–adrenal axis activity: implications for the integration of limbic inputs, J. Neurosci. 27 (2007) 2025–2034.
[8] A. Cudennec, G. Bonvento, D. Duverger, P. Lacombe, J. Seylaz, E.T. MacKenzie, Effects of dorsal raphe nucleus stimulation on cerebral blood flow and flow-metabolism coupling in the conscious rat, Neuroscience 55 (1993) 395–401.
[9] C.W. Davies, J.H. Crosby, R.L. Mullins, Z.C. Traill, P. Anslow, R.J. Davies, J.R. Stradling, Case control study of cerebrovascular damage defined by magnetic resonance imaging in patients with OSA and normal matched control subjects, Sleep 24 (2001) 715–720.
[10] J.A. Dempsey, S.C. Veasey, B.J. Morgan, C.P. O'Donnell, Pathophysiology of sleep apnea, Physiol. Rev. 90 (2010) 47–112.
[11] J.A. Detre, D.C. Alsop, L.R. Vives, L. Maccotta, J.W. Teener, E.C. Raps, Noninvasive MRI evaluation of cerebral blood flow in cerebrovascular disease, Neurology 50 (1998) 633–641.
[12] J.H. Ficker, H. Feistel, C. Moller, M. Merkl, S. Dertinger, W. Siegfried, E.G. Hahn, Changes in regional CNS perfusion in obstructive sleep apnea syndrome: initial SPECT studies with injected nocturnal 99mTc-HMPAO, Pneumologie 51 (1997) 926–930.
[13] D. Gaffan, Loss of recognition memory in rats with lesions of the fornix, Neuropsychologia 10 (1972) 327–341.
[14] N.R. Gonzalez, W.J. Boscardin, T. Glenn, F. Vinuela, N.A. Martin, Vasospasm probability index: a combination of transcranial doppler velocities, cerebral blood flow, and clinical risk factors to predict cerebral vasospasm after aneurysmal subarachnoid hemorrhage, J. Neurosurg. 107 (2007) 1101–1112.
[15] L.A. Henderson, M.A. Woo, P.M. Macey, K.E. Macey, R.C. Frysinger, J.R. Alger, F. Yan-Go, R.M. Harper, Neural responses during Valsalva maneuvers in obstructive sleep apnea syndrome, J. Appl. Physiol. 94 (2003) 1063–1074.
[16] R.S. Johansson, K.J. Cole, Sensory-motor coordination during grasping and manipulative actions, Curr. Opin. Neurobiol. 2 (1992) 815–823.
[17] L. Kheirandish-Gozal, A. Khalyfa, D. Gozal, R. Bhattacharjee, Y. Wang, Endothelial dysfunction in children with obstructive sleep apnea is associated with epigenetic changes in the eNOS gene, Chest 143 (2013) 971–977.
[18] N. Koshiya, D. Huangfu, P.G. Guyenet, Ventrolateral medulla and sympathetic chemoreflex in the rat, Brain Res. 609 (1993) 174–184.

[19] R. Kumar, B.V. Birrer, P.M. Macey, M.A. Woo, R.K. Gupta, F.L. Yan-Go, R.M. Harper, Reduced mammillary body volume in patients with obstructive sleep apnea, Neurosci. Lett. 438 (2008) 330–334.
[20] R. Kumar, A.S. Chavez, P.M. Macey, M.A. Woo, F.L. Yan-Go, R.M. Harper, Altered global and regional brain mean diffusivity in patients with obstructive sleep apnea, J. Neurosci. Res. 90 (2012) 2043–2052.
[21] R. Kumar, H.D. Nguyen, P.M. Macey, M.A. Woo, R.M. Harper, Dilated basilar arteries in patients with congenital central hypoventilation syndrome, Neurosci. Lett. 467 (2009) 139–143.
[22] S.I. Letovsky, S.H. Whitehead, C.H. Paik, G.A. Miller, J. Gerber, E.H. Herskovits, T.K. Fulton, R.N. Bryan, A brain image database for structure/function analysis, Am. J. Neuroradiol. 19 (1998) 1869–1877.
[23] P.M. Macey, R. Kumar, M.A. Woo, E.M. Valladares, F.L. Yan-Go, R.M. Harper, Brain structural changes in obstructive sleep apnea, Sleep 31 (2008) 967–977.
[24] P.M. Macey, R. Kumar, F.L. Yan-Go, M.A. Woo, R.M. Harper, Sex differences in white matter alterations accompanying obstructive sleep apnea, Sleep 35 (2012) 1603–1613.
[25] J.S. Meyer, Y. Ishikawa, T. Hata, I. Karacan, Cerebral blood flow in normal and abnormal sleep and dreaming, Brain Cogn. 6 (1987) 266–294.
[26] B.D. Murphy, X. Chen, T.Y. Lee, Serial changes in CT cerebral blood volume and flow after 4 hours of middle cerebral occlusion in an animal model of embolic cerebral ischemia, Am. J. Neuroradiol. 28 (2007) 743–749.
[27] H.F. Ni, J.X. Zhang, R.M. Harper, Cardiovascular-related discharge of periaqueductal gray neurons during sleep-waking states, Brain Res. 532 (1990) 242–248.
[28] H.F. Ni, J.X. Zhang, R.M. Harper, Respiratory-related discharge of periaqueductal gray neurons during sleep-waking states, Brain Res. 511 (1990) 319–325.
[29] K. Oishi, A. Faria, H. Jiang, X. Li, K. Akhter, J. Zhang, J.T. Hsu, M.I. Miller, P.C. van Zijl, M. Albert, C.G. Lyketsos, R. Woods, A.W. Toga, G.B. Pike, P. Rosa-Neto, A. Evans, J. Mazziotta, S. Mori, Atlas-based whole brain white matter analysis using large deformation diffeomorphic metric mapping: application to normal elderly and Alzheimer's disease participants, NeuroImage 46 (2009) 486–499.
[30] E.K. Pae, P. Chien, R.M. Harper, Intermittent hypoxia damages cerebellar cortex and deep nuclei, Neurosci. Lett. 375 (2005) 123–128.
[31] V.K. Somers, M.E. Dyken, M.P. Clary, F.M. Abboud, Sympathetic neural mechanisms in obstructive sleep apnea, J. Clin. Invest. 96 (1995) 1897–1904.
[32] J.J. Strouse, C.S. Cox, E.R. Melhem, H. Lu, M.A. Kraut, A. Razumovsky, K. Yohay, P.C. van Zijl, J.F. Casella, Inverse correlation between cerebral blood flow measured by continuous arterial spin-labeling (CASL) MRI and neurocognitive function in children with sickle cell anemia (SCA), Blood 108 (2006) 379–381.
[33] V.S. Ten, D.J. Pinsky, Endothelial response to hypoxia: physiologic adaptation and pathologic dysfunction, Curr. Opin. Crit. Care 8 (2002) 242–250.
[34] F. Urbano, F. Roux, J. Schindler, V. Mohsenin, Impaired cerebral autoregulation in obstructive sleep apnea, J. Appl. Physiol. 105 (2008) 1852–1857.
[35] J. Wang, Y. Zhang, R.L. Wolf, A.C. Roc, D.C. Alsop, J.A. Detre, Amplitude-modulated continuous arterial spin-labeling 3.0-T perfusion MR imaging with a single coil: feasibility study, Radiology 235 (2005) 218–228.
[36] W. Wang, S.R. Bradley, G.B. Richerson, Quantification of the response of rat medullary raphe neurones to independent changes in pH(o) and $P(CO_2)$, J. Physiol. 540 (2002) 951–970.
[37] K. Yamashita, S. Kobayashi, S. Yamaguchi, M. Kitani, T. Tsunematsu, Effect of smoking on regional cerebral blood flow in the normal aged volunteers, Gerontology 34 (1988) 199–204.
[38] B. Yan, L. Li, S.W. Harden, D. Gozal, Y. Lin, W.B. Wead, R.D. Wurster, Z.J. Cheng, Chronic intermittent hypoxia impairs heart rate responses to AMPA and NMDA and induces loss of glutamate receptor neurons in nucleus ambiguous of F344 rats, Am. J. Physiol. Regul. Integr. Comp. Physiol. 296 (2009) R299–R308.